

SUPPLEMENTARY ONLINE DATA

Structure-guided optimization of protein kinase inhibitors reverses aminoglycoside antibiotic resistance

Peter J. Stogios^{*,†}, Peter Spanogiannopoulos^{‡,¶}, Elena Evdokimova^{*,†}, Olga Egorova^{*}, Tushar Shakya^{‡,§}, Nick Todorovic^{§,¶}, Alfredo Capretta^{§,¶}, Gerard D. Wright^{‡,¶} and Alexei Savchenko^{*,†,*}

^{*}Department of Chemical Engineering and Applied Chemistry, University of Toronto, Toronto, Ontario, M5G 1L6, Canada

[†]Center for Structural Genomics of Infectious Diseases (CSGID)

[‡]Department of Biochemistry and Biomedical Sciences, McMaster University, Hamilton, Ontario, L8N 3Z5, Canada

[§]Department of Chemistry and Chemical Biology, McMaster University, Hamilton, Ontario, L8S 4M1, Canada

[¶]M. G. DeGrootte Institute for Infectious Disease Research, McMaster University, Hamilton, Ontario, L8S 3Z5, Canada

*Corresponding author: Alexei Savchenko, Associate Professor, 200 College St, Room 420B, Department of Chemical Engineering and Applied Chemistry, University of Toronto, Toronto, Ontario, M5G 1L6, Canada. email: alexei.savchenko@utoronto.ca, phone: +1-416-978-3925, fax: +1-416-971-2106.

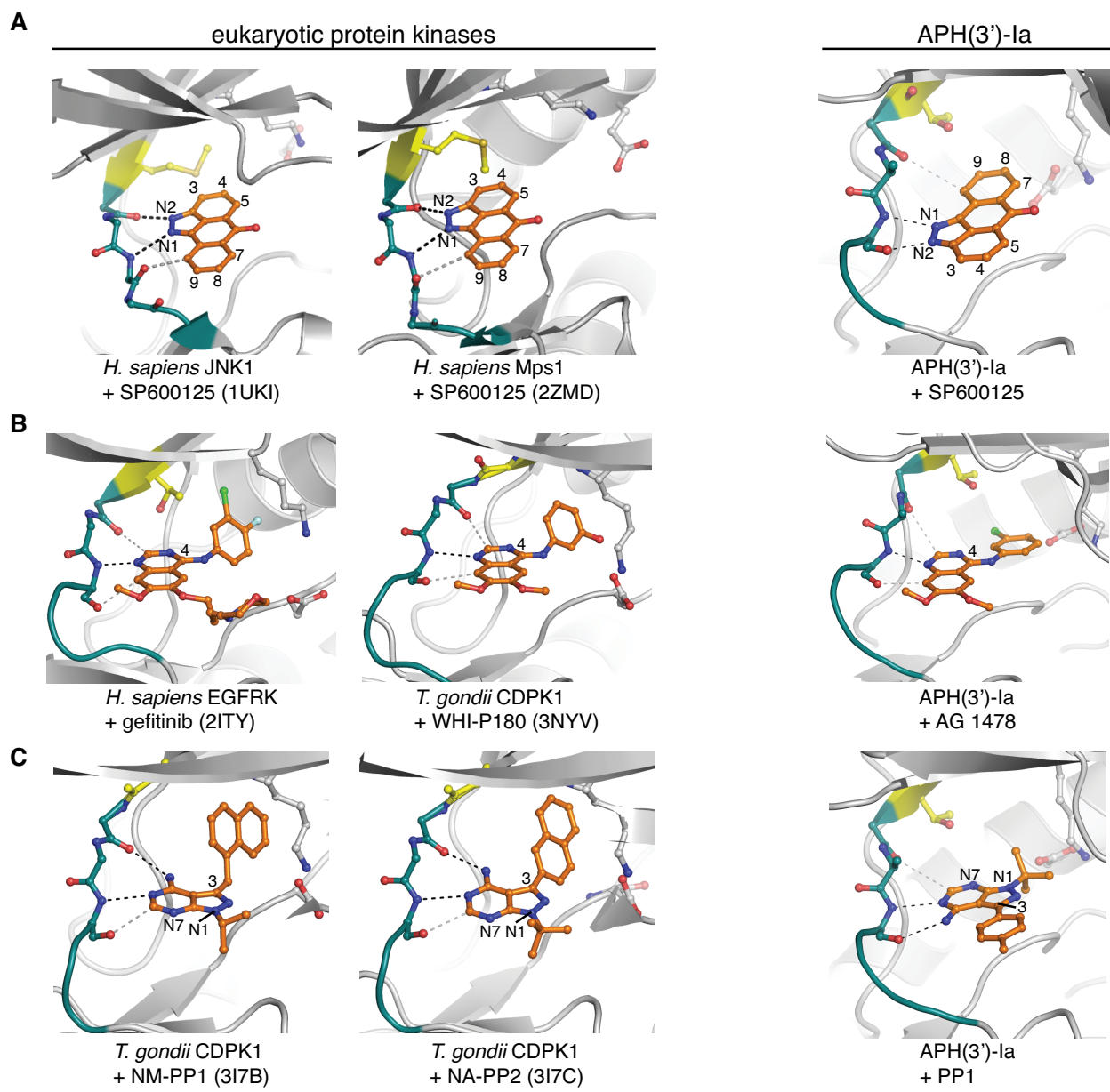


Figure S1 Comparison of binding mode of SP600125, 4-anilinoquinazoline compounds, and pyrazolopyrimidine compounds between ePKs (two left panels) and APH(3')-Ia (right panels).

A) Structures of SP600125 complexes. B) Structures of 4-anilinoquinazoline inhibitor complexes. C) Structures of C3-derivatized PP inhibitor complexes. For each of the three inhibitor classes, structures shown are representative of all complexes found in search of PDB in that the inhibitor is bound in the same orientation and interactions between the inhibitor and the hinge region of the ePKs are conserved within the inhibitor class.

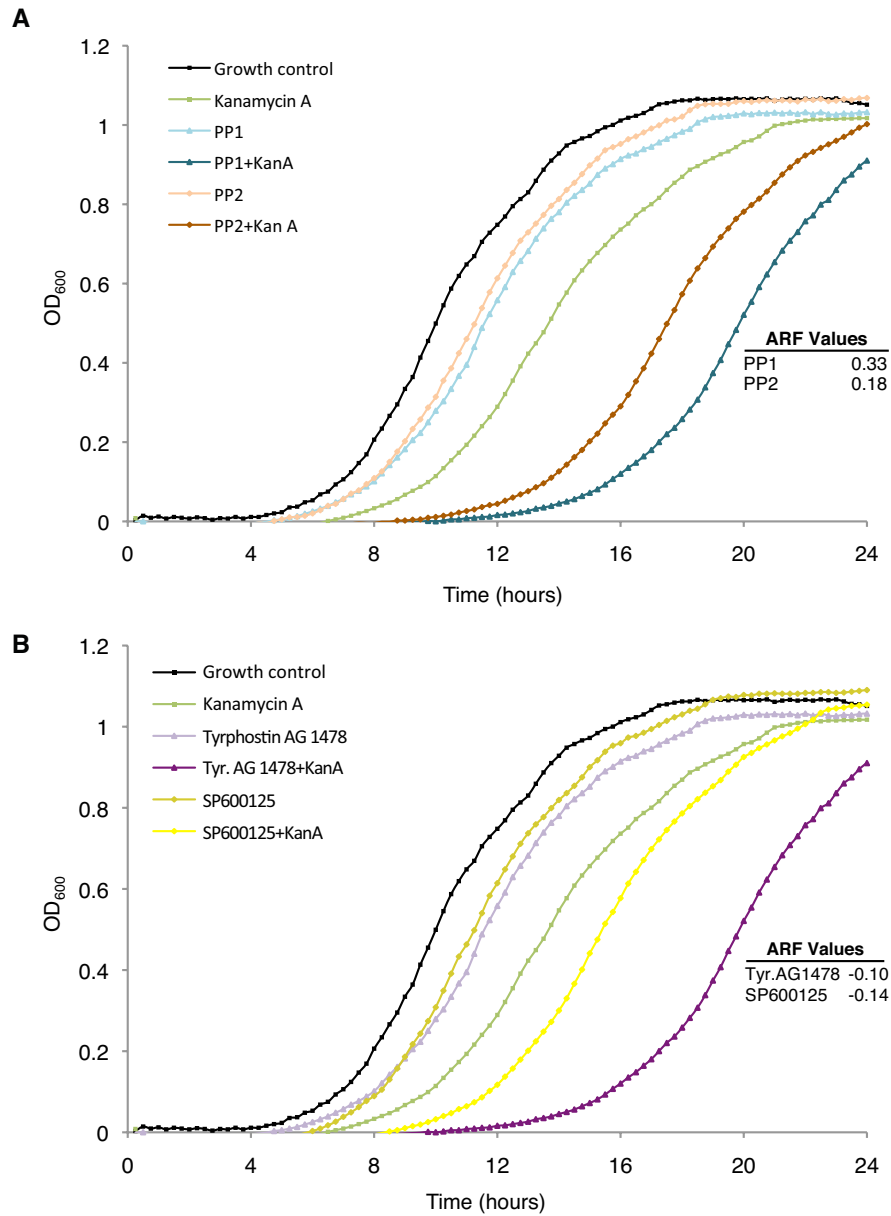


Figure S2 Growth of *E. coli* expressing *aphA1* in the presence of PP1, PP2, AG 1478 and SP600125.

A) Growth curves of *E. coli* $\Delta tolC \Delta bamB$ containing pET22-*aphA1* grown in the presence of PP1 alone (64 μ M; light blue triangles), PP1 (64 μ M) in combination with kanamycin A at $\frac{1}{4}$ MIC (dark blue triangles), PP2 alone (64 μ M; tan diamonds) and PP2 (64 μ M) in combination with kanamycin A at $\frac{1}{4}$ MIC (brown diamonds). B) Growth curves of *E. coli* $\Delta tolC \Delta bamB$ containing pET22-*aph(3')-Ia* grown in the presence of Tyrphostin AG 1478 alone (64 μ M, light blue triangles), Tyrphostin AG 1478 (64 μ M) in combination with kanamycin A at $\frac{1}{4}$ MIC (dark blue triangles), SP600125 alone (64 μ M; tan diamonds), and SP600125 (64 μ M) in combination with kanamycin A at $\frac{1}{4}$ MIC (brown diamonds). For both plots is shown are normal growth control (black squares) and kanamycin A at $\frac{1}{4}$ MIC control (green squares). Inset: corresponding ARF values for compounds.

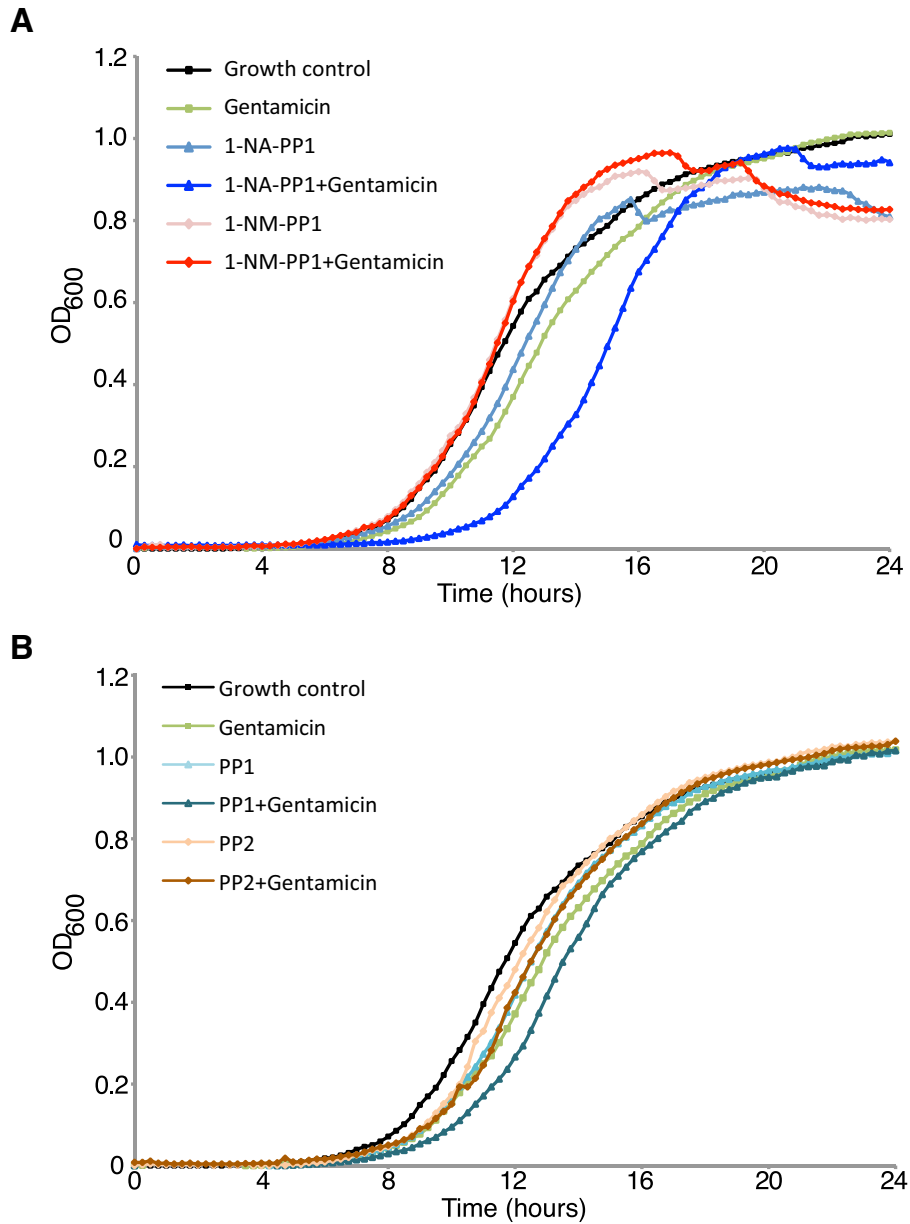


Figure S3 Growth of *E. coli* expressing aminoglycoside acetyltransferase *aac(3)-Ia* in the presence of pyrazolopyrimidines

A) Growth curves of *E. coli* $\Delta tolC \Delta bamB$ containing pGDP4-*aac(3)-Ia* grown in the presence of 1-NA-PP1 alone (64 μ M; light blue triangles), 1-NA-PP1 (64 μ M) in combination with gentamicin at $\frac{1}{4}$ MIC (dark blue triangles), 1-NM-PP1 alone (32 μ M; pink diamonds) and PP2 (64 μ M) in combination with gentamicin at $\frac{1}{4}$ MIC (red diamonds). B) Growth curves of *E. coli* $\Delta tolC \Delta bamB$ containing pGDP4-*aac(3)-Ia* grown in the presence of PP1 alone (64 μ M, light teal triangles), PP1 (64 μ M) in combination with gentamicin at $\frac{1}{4}$ MIC (dark teal triangles), PP2 alone (64 μ M; tan diamonds), and PP2 (64 μ M) in combination with gentamicin at $\frac{1}{4}$ MIC (brown diamonds). For both plots also shown is normal growth control (black squares) and in the presence of gentamicin at $\frac{1}{4}$ MIC control (green squares).

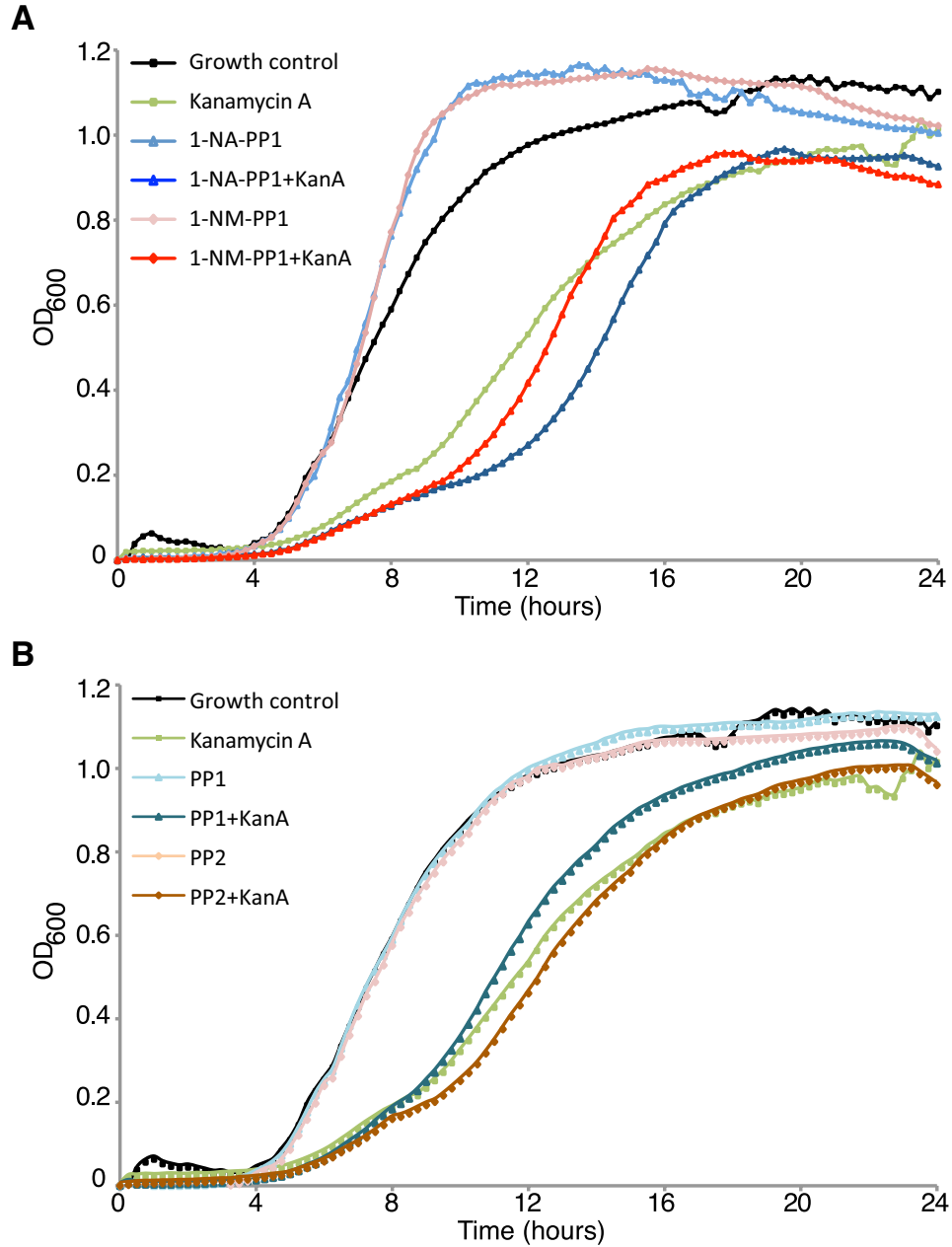


Figure S4 Growth of wildtype *E. coli* expressing *aphA1* in the presence of pyrazolopyrimidines

A) Growth curves of wildtype *E. coli* containing pET22-*aphA1* grown in the presence of 1-NA-PP1 alone (64 μ M; light blue triangles), 1-NA-PP1 (64 μ M) in combination with kanamycin A at $\frac{1}{4}$ MIC (dark blue triangles), 1-NM-PP1 alone (32 μ M; pink diamonds) and PP2 (64 μ M) in combination with kanamycin A at $\frac{1}{4}$ MIC (red diamonds). B) Growth curves of *E. coli* containing pET22-*aphA1* grown in the presence of PP1 alone (64 μ M, light teal triangles), PP1 (64 μ M) and in combination with kanamycin A at $\frac{1}{4}$ MIC (dark teal triangles), PP2 alone (64 μ M; tan diamonds), and PP2 (64 μ M) in combination with kanamycin A at $\frac{1}{4}$ MIC (brown diamonds). For both plots also shown is normal growth control (black squares) and in the presence of kanamycin A at $\frac{1}{4}$ MIC control (green squares).